Electronic Supporting Information

Distinct Photomechanical Responses of Two new 1,3-Dimethylbarbituric Acid Derivative Crystals

Sayak Nag,[a] Franziska Emmerling,[b] Srinu Tothadi,[c] Biswajit Bhattacharya,[b] Soumyajit Ghosh*[a]*

[a]Department of Chemistry, SRM Institute of Science and Technology, Kattankulathur 603 203, Tamil Nadu, India.

[b]BAM Federal Institute for Materials Research and Testing, Richard-Willstätter-Str. 11, 12489 Berlin, Germany.

[c]Analytical and Environmental Sciences Division and Centralized Instrumentation Facility, CSIR-Central Salt and Marine Chemicals Research Institute, Gijubhai Badheka Marg, Bhavnagar-364002 (India).

* Email: soumyajitghosh89@gmail.com

biswajit.bhattacharya@bam.de

Synthesis Scheme

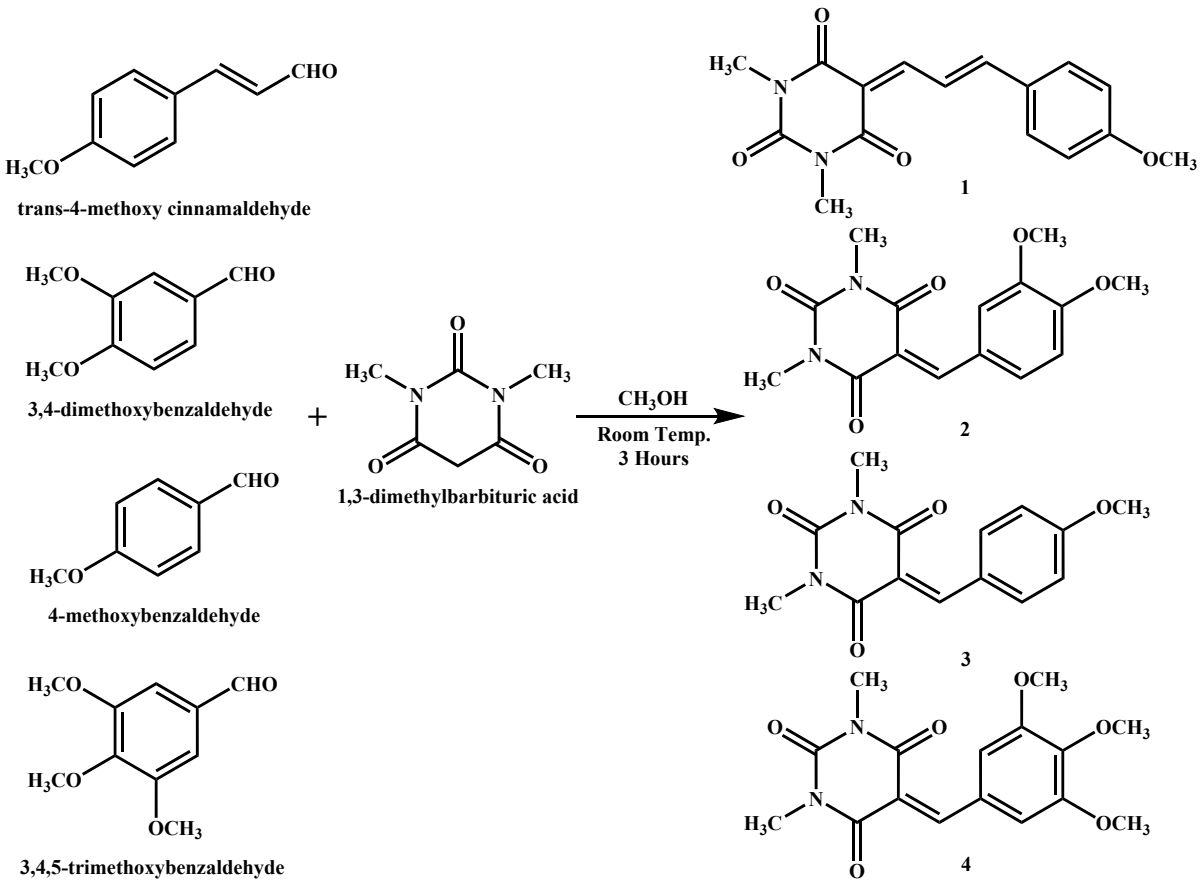

Scheme S1. Synthesis route of compounds **1-4**.

Compounds **1-4** were synthesized using a reported procedure by dissolving 1,3-Dimethylbarbituric acid (1 mmol) in a 100 ml round bottom-flask containing 15 ml of methanol, and to the resultant solution trans-4-methoxycinnamaldehyde (1 mmol), 3,4-dimethoxybenzaldehdye (1 mmol), 4-methoxy benzaldehyde (1 mmol) and 3,4,5-trimethoxy benzaldehyde (1 mmol) were added respectively and stirred for 3 hours under the ambient condition to obtain precipitates of **1-4 (Scheme S1)** with decent yield (Compound **1**: ~85%, Compound **2**: ~47%, Compound **3**: ~55% and Compound **4**: ~63%).

Recrystallisation Table

Table S1: Results from the recrystallisation of Compond **1** and **2** from one solvent or mixture of solvents.

S.No.	Solvents	Compound 1	Compound 2
1.	Dichloromethane + n-Hexane (1:1)	Powder	Powder
2.	Dichloromethane + Methanol (1:1)	Powder	Powder
3.	Ethyl Acetate + n-Hexane (1:1)	Powder	Powder
4.	Ethyl Acetate + Methanol (1:1)	Powder	Powder
5.	Ethyl Acetate	Powder	Powder
6.	Acetonitrile	Powder	Fine Needles
7.	Acetone	Fine Needles	Fine Needles
8.	Methanol + Chloroform (1:1)	Fine Needles	Powder
9.	Chloroform	Powder	Powder

Nuclear Magnetic Resonance (NMR) Analysis.

^{1}H NMR spectra of both Crystal **1** and Crystal **2** were taken in $CDCl_3$ solvent. ^{1}H NMR spectra were collected under standard conditions. Chemical shifts (δ) were reported in parts per million (ppm) and referenced to the residual solvent peak at 7.26 ppm for the $CDCl_3$ solvent peak and 1.60 ppm for the $CDCl_3$ water peak.

Crystal 1: (^{1}H NMR – 500 MHz, $CDCl_3$, TMS) δ 3.39 ppm (d, J= 1.9 Hz, 6H, N-methyl-H), δ 3.88 ppm (s, 3H, methoxy-H), δ 6.94 ppm (d, J= 10 Hz, 2H, aromatic-H(ortho)), δ 7.41 ppm (d, J= 15.3 Hz, 1H, benzylic-H), δ 7.65 ppm (d, J= 10 Hz, 2H, aromatic-H(meta)), δ 8.20 ppm (d, J= 12.1 Hz, 1H, vinylic-H), δ 8.49 ppm (dd, J= 15.2, 12.2 Hz, 1H, allylic-H) (Fig. S1).

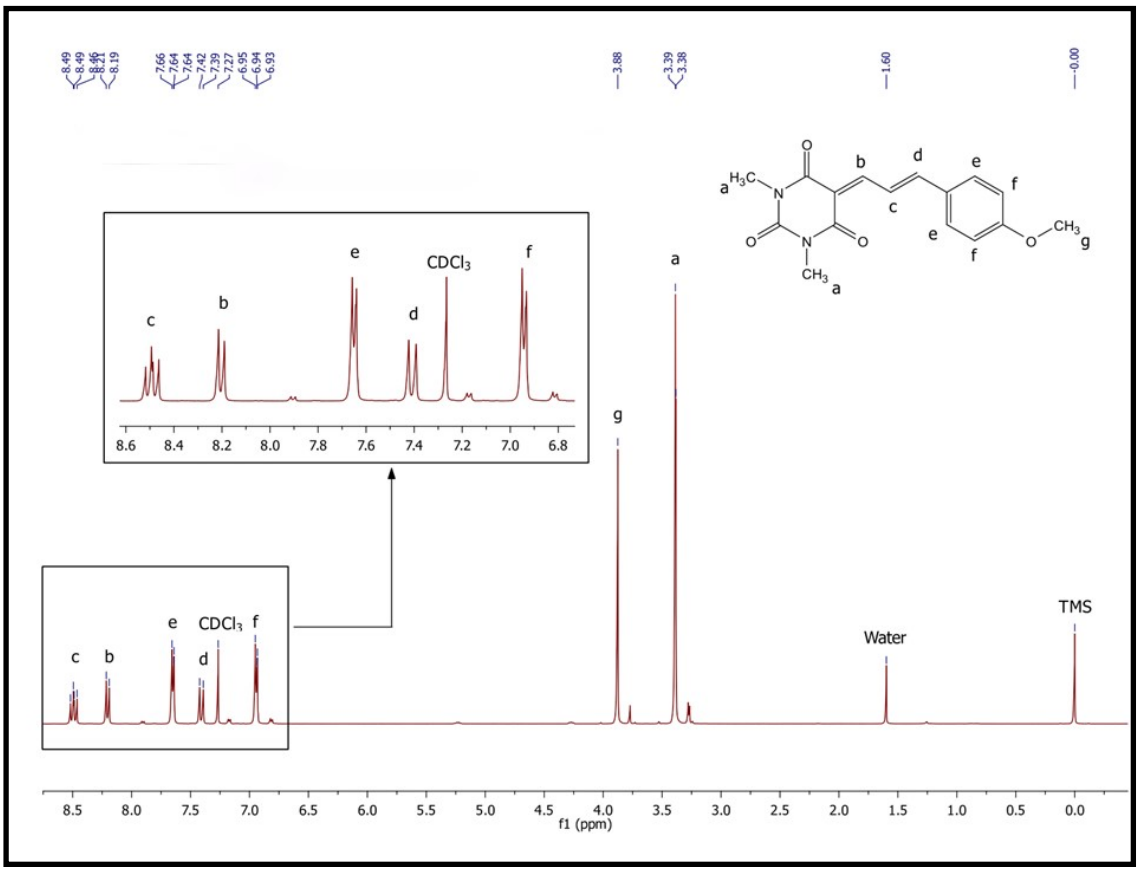

Figure S1. ^{1}H NMR spectrum of Crystal **1** (solvent: $CDCl_3$, peak at 7.26 ppm).

Crystal 2: (^{1}H NMR – 500 MHz, $CDCl_3$, TMS) δ 3.41 ppm (d, J= 9.2 Hz, 6H, N-methyl-H), δ 3.99 ppm (s, 6H, methoxy-H), δ 6.96 (d, J= 8.4 Hz, 1H, aromatic-H), δ 7.79 ppm (d, J= 8.3

Hz, 1H, aromatic-H), δ 8.40 ppm (s, 1H, aromatic-H), δ 8.50 ppm (s, 1H, vinylic-H) (Fig. S2).

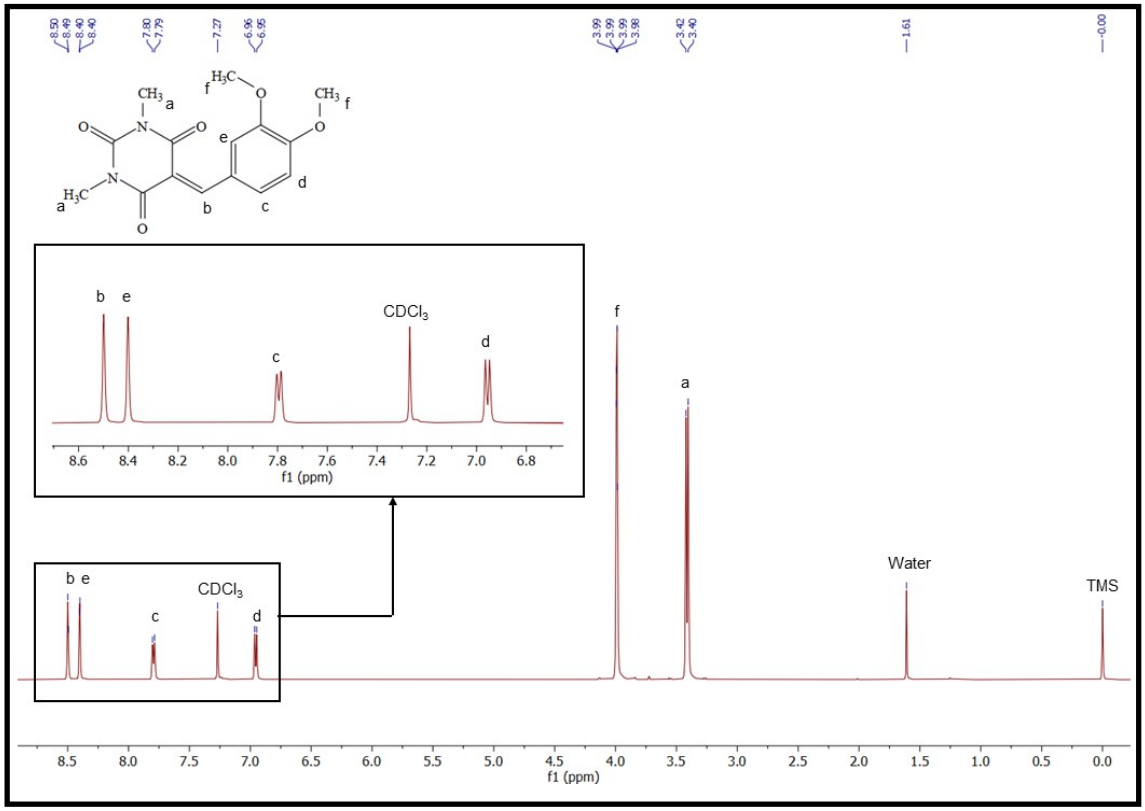

Figure S2. ^{1}H NMR spectrum of Crystal **2** (solvent: $CDCl_3$, peak at 7.26 ppm).

Compound 3: (^{1}H NMR – 500 MHz, $CDCl_3$, TMS) δ 3.41 ppm (d, 6H, 11 Hz, N-methyl-H), δ 3.91 (s, 3H, methoxy-H), δ 6.98 ppm (d, 2H, 9 Hz, aromatic-H), δ 8.33 ppm (d, 2H, 8.8 Hz, aromatic-H), δ 8.52 ppm (s, 1H, vinylic-H) (Fig. S3).

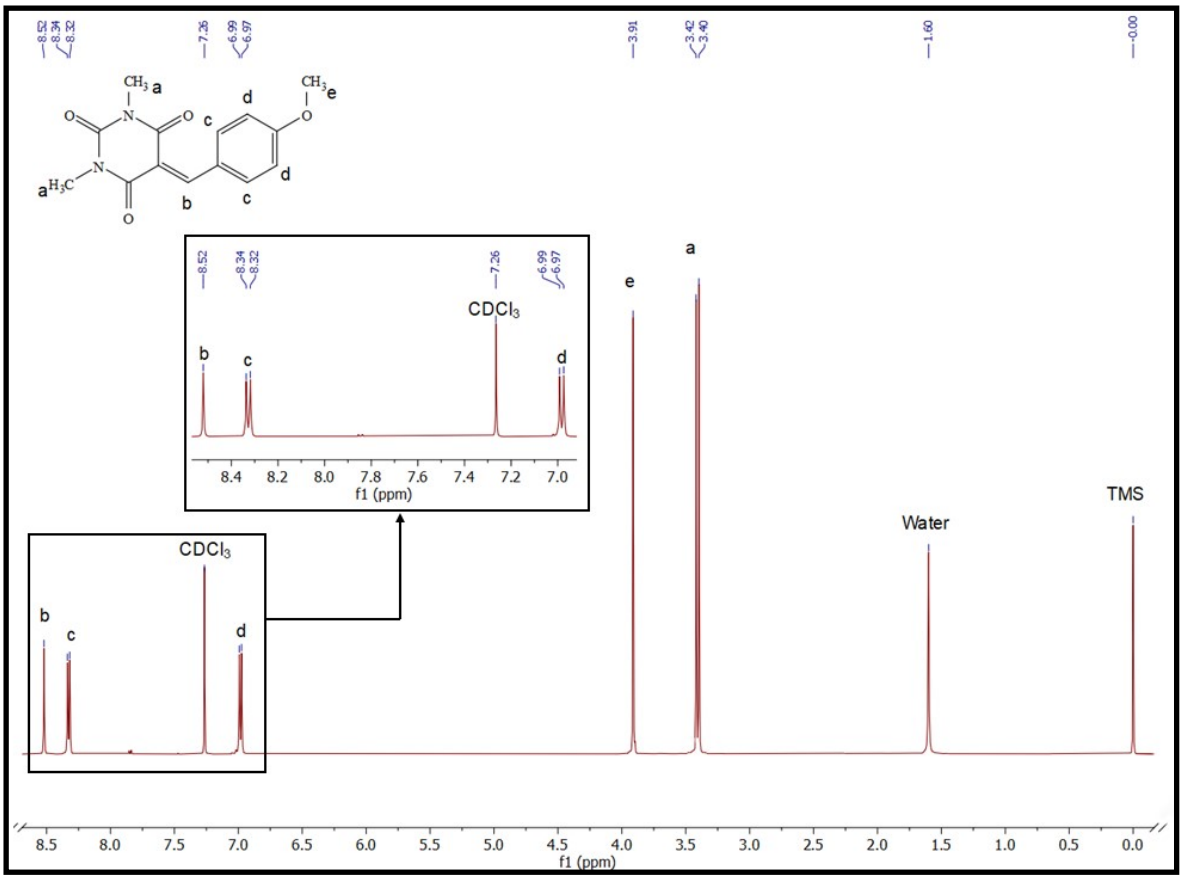

Figure S3. ^{1}H NMR spectrum of compound **3** (solvent: $CDCl_3$, peak at 7.26).

Compound 4: (^{1}H NMR – 500 Mhz, $CDCl_3$, TMS) δ 3.42 ppm (d, 6H, 13.7 Hz, N-methyl-H), δ 3.94 ppm (s, 6H, methoxy-H), δ 3.99 (s, 3H, methoxy-H), δ 7.72 ppm (s, 2H, aromatic-H), δ 8.47 ppm (s, 1H, vinylic-H) (Fig. S4).

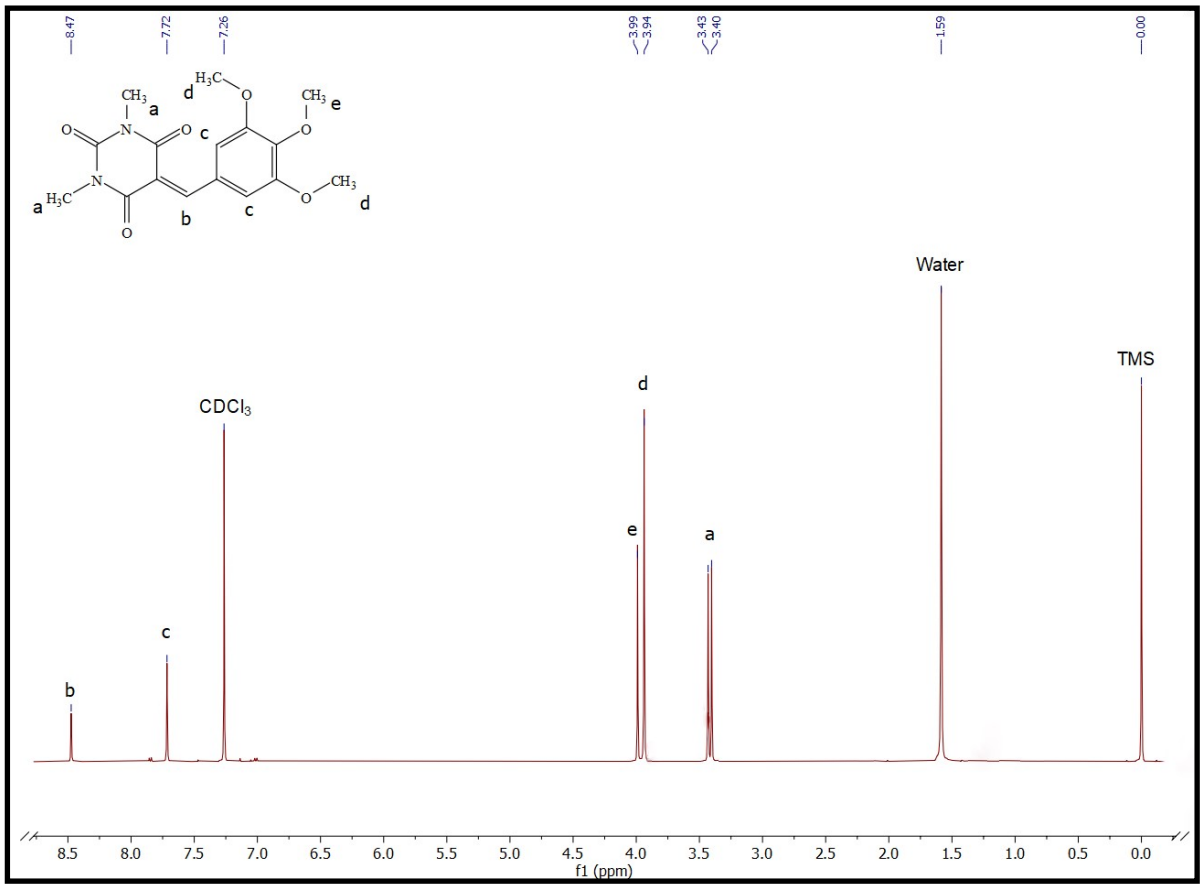

Figure S4. ^{1}H NMR spectrum of compound **4** (solvent: $CDCl_3$, peak at 7.26).

Differential Scanning Calorimetry (DSC) Analysis.

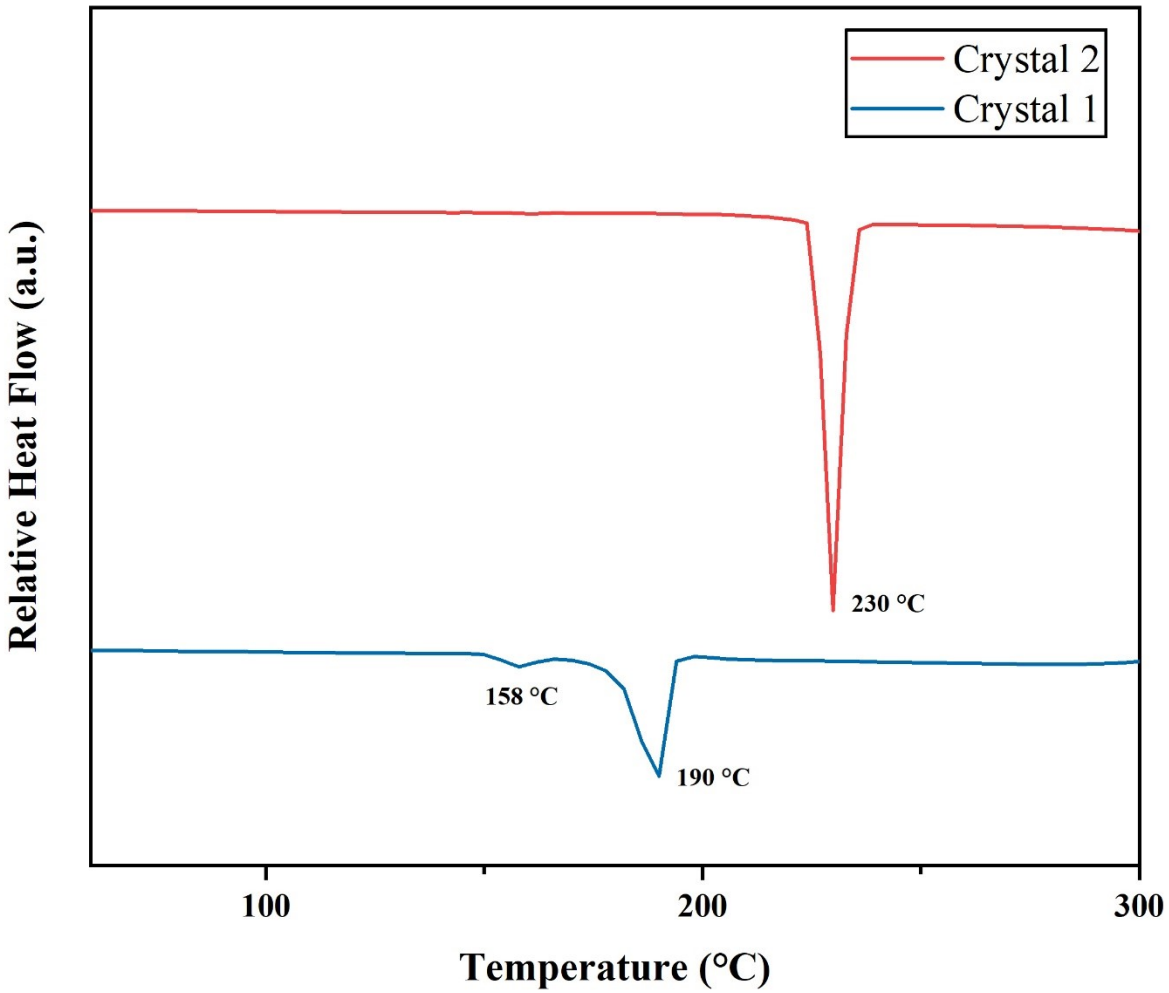

Figure S5. Comparative Differential Scanning Calorimetry (DSC) diagram of Crystal **1** and **2**.

Photosalient Bursting and Jumping Images of Crystal 2.

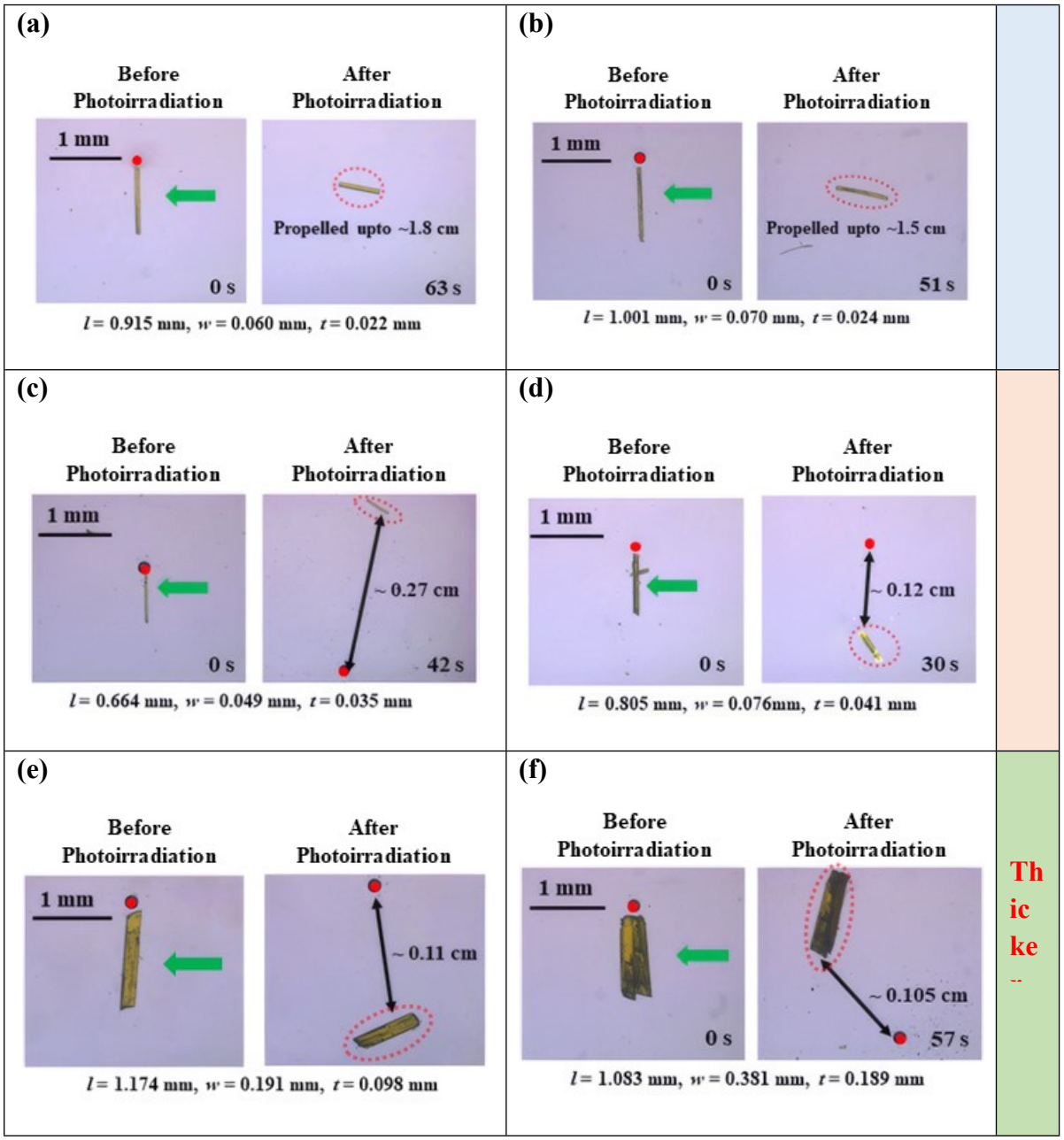

Figure S6. Photosalient bursting and jumping off images of crystal **2 (a-b)** for thinner crystals, **(c-d)** for moderately thicker crystals, **(e-f)** for relatively thicker crystals. Red dots were placed to designate the initial position of the crystals and Green arrow designate the direction of the light source. The broken fragments are highlighted with red dotted circle.

Kinematic Study Data of Crystal 2.

Table S2: Photosalient responses of crystals of different dimensions.

S. No.	Dimensions			Photosalient Effect	Propelled Distance
	Thickness *(t)*	Length *(l)*	Width (w)		
1.	0.020 mm	1.092 mm	0.047 mm	Fragmentation of the crystal followed by jumping off to a certain distance.	~2.0 cm
2.	0.022 mm	0.915 mm	0.060 mm		~1.8 cm
3.	0.024 mm	1.001 mm	0.070 mm		~1.5 cm
4.	0.025 mm	0.769 mm	0.071 mm		~1.1 cm
5.	0.035 mm	0.664 mm	0.049 mm		~0.27 cm
6.	0.039 mm	0.813 mm	0.084 mm		~0.19 cm
7.	0.041 mm	0.805 mm	0.076 mm		~0.12 cm
8.	0.045 mm	1.115 mm	0.080 mm		~0.126 cm
9.	0.053 mm	0.985 mm	0.084 mm		~0.114 cm
10.	0.098 mm	1.174 mm	0.191		~1.1 cm
11.	0.189 mm	1.083 mm	0.381 mm		~0.105 cm

Photosalient Bending Images of Crystal 1.

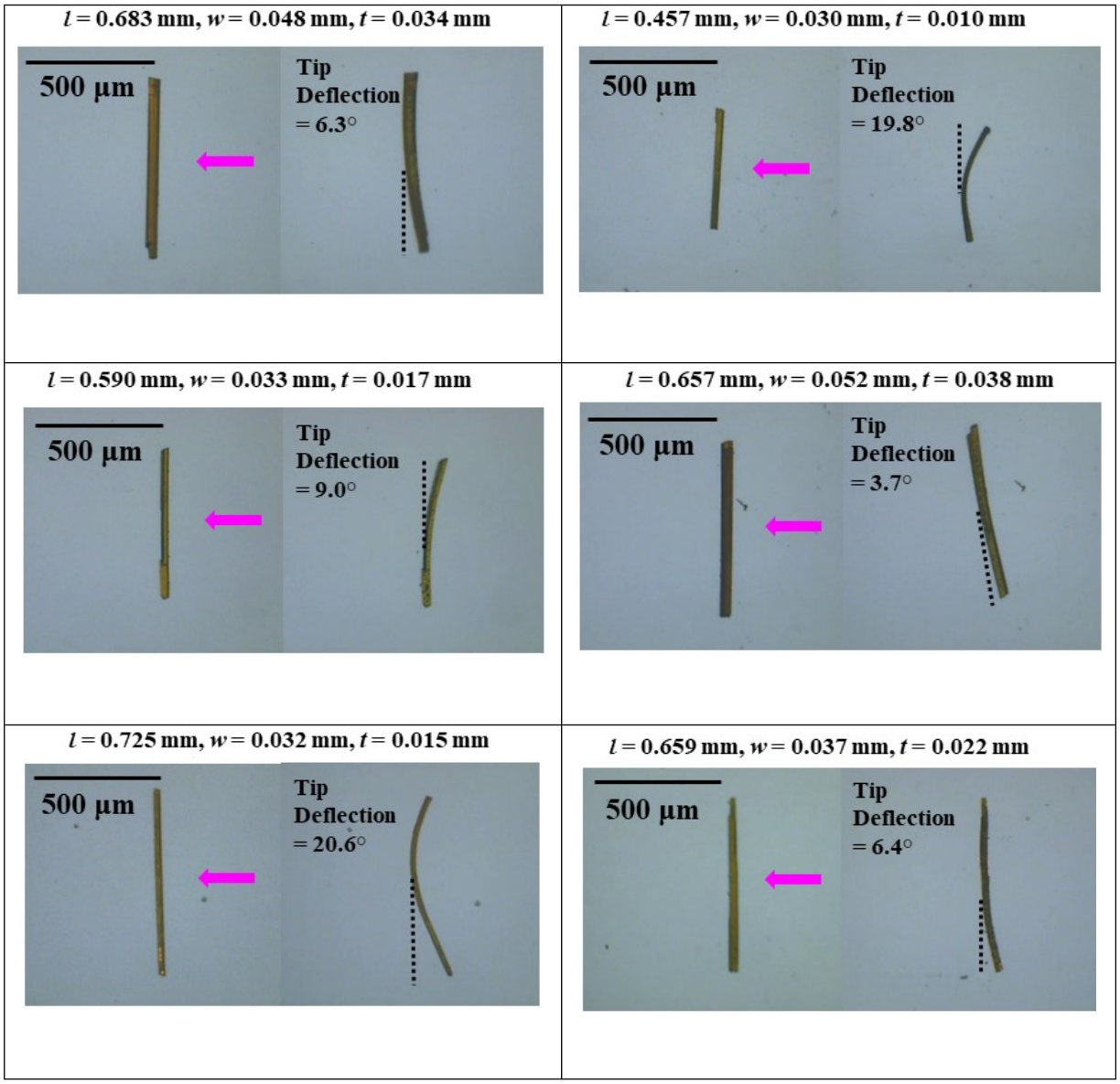

Figure S7. Photosalient bending images of a set of different dimension crystals of **1**. Purple arrows denote the direction of the LASER source.

Energy Framework Calculations

The energy framework calculations[1,2] relating to intermolecular interactions of crystals **1** and **2** were performed using the software suite Crystal-Explorer based on B3LYP/6-31G(d,p) molecular wavefunctions calculated using the CIF files. For calculations, the hydrogen atoms were normalized to standard neutron diffraction values. The energy frameworks constructed were based on the crystal symmetry and total interaction energy components of which included electrostatic, polarization, dispersion and exchange repulsion components scaled by 1.057,

0.740, 0.871 and 0.618, respectively. The interaction energies below 5 kJ.mol^{-1} are omitted for clarity and the cylinder thickness is proportional to the intermolecular interaction energies along the parallel vector passing through the cylinder.

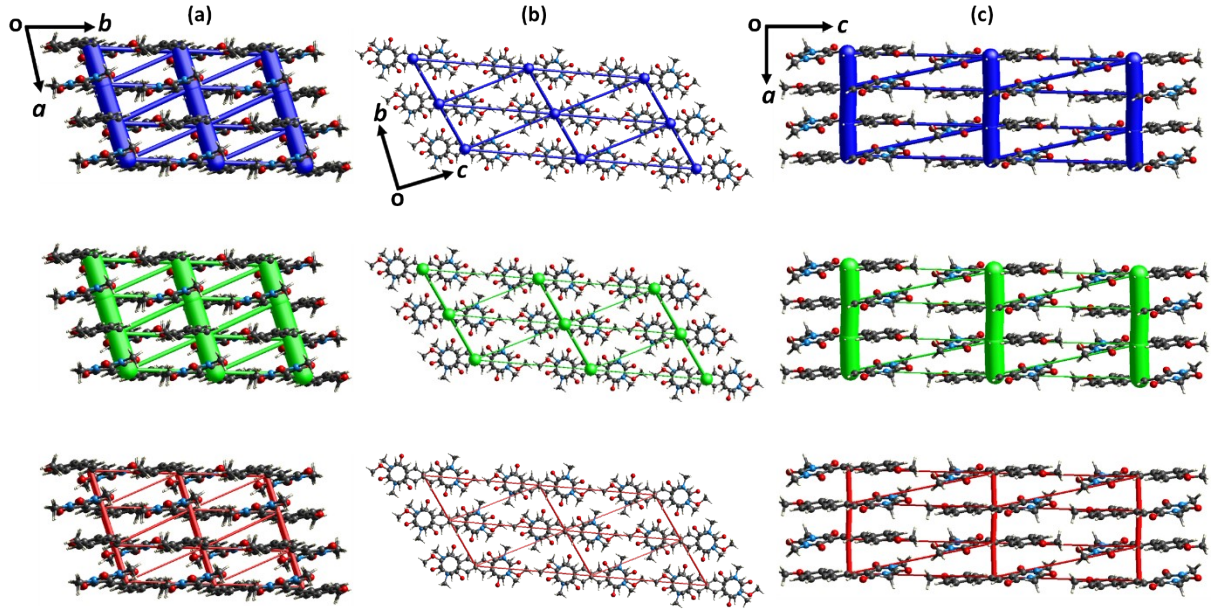

Figure. S8. Visualization of energy frameworks showing total interaction energy (top, blue), dispersion (middle, green) and electrostatic (below, red) components crystal **1**, in the **(a)** (001), **(b)** (100) and **(c)** (010) faces, respectively. The energy threshold is 5 kJ.mol^{-1}.

Table S3: (a) Molecular structure pairs and **(b)** the interaction energies (kJ.mol^{-1}) obtained from energy frameworks calculation for crystal **1**. Scale factors are in the lower table.

(a)

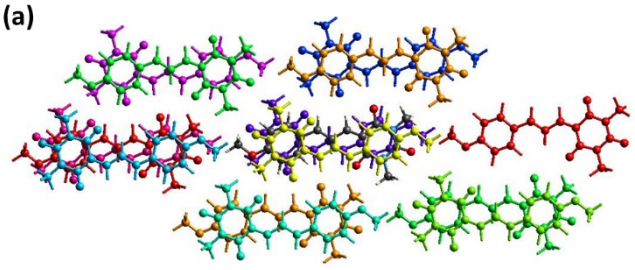

(b) Interaction Energies (kJ/mol)
R is the distance between molecular centroids (mean atomic position) in Å.

Total energies, only reported for two benchmarked energy models, are the sum of the four energy components, scaled appropriately (see the scale factor table below)

N	Symop	R	Electron Density	E_ele	E_pol	E_dis	E_rep	E_tot
2	x, y, z	17.09	B3LYP/6-31G(d,p)	-7.1	-2.1	-7.1	0.0	-15.3
2	x, y, z	8.02	B3LYP/6-31G(d,p)	-7.5	-3.2	-19.5	12.6	-19.5
1	-x, -y, -z	3.37	B3LYP/6-31G(d,p)	-21.5	-2.4	-103.6	55.0	-80.7
1	-x, -y, -z	13.63	B3LYP/6-31G(d,p)	-7.9	-2.7	-9.6	0.0	-18.8
2	x, y, z	13.95	B3LYP/6-31G(d,p)	-1.6	-0.7	-6.9	0.0	-8.2
1	-x, -y, -z	7.98	B3LYP/6-31G(d,p)	-6.7	-2.0	-22.2	13.1	-19.8
1	-x, -y, -z	17.65	B3LYP/6-31G(d,p)	1.0	-0.5	-4.0	0.0	-2.8
1	-x, -y, -z	7.30	B3LYP/6-31G(d,p)	-10.4	-4.9	-28.2	20.4	-26.6
1	-x, -y, -z	3.88	B3LYP/6-31G(d,p)	-23.1	-2.8	-96.8	52.5	-78.4
1	-x, -y, -z	15.34	B3LYP/6-31G(d,p)	3.4	-0.6	-3.0	0.0	0.6
1	-x, -y, -z	18.94	B3LYP/6-31G(d,p)	0.3	-0.4	-3.2	0.0	-2.8

Scale factors for benchmarked energy models
See Mackenzie et al. IUCrJ (2017)

Energy Model	k_ele	k_pol	k_disp	k_rep
CE-HF ... HF/3-21G electron densities	1.019	0.651	0.901	0.811
CE-B3LYP ... B3LYP/6-31G(d,p) electron densities	1.057	0.740	0.871	0.618

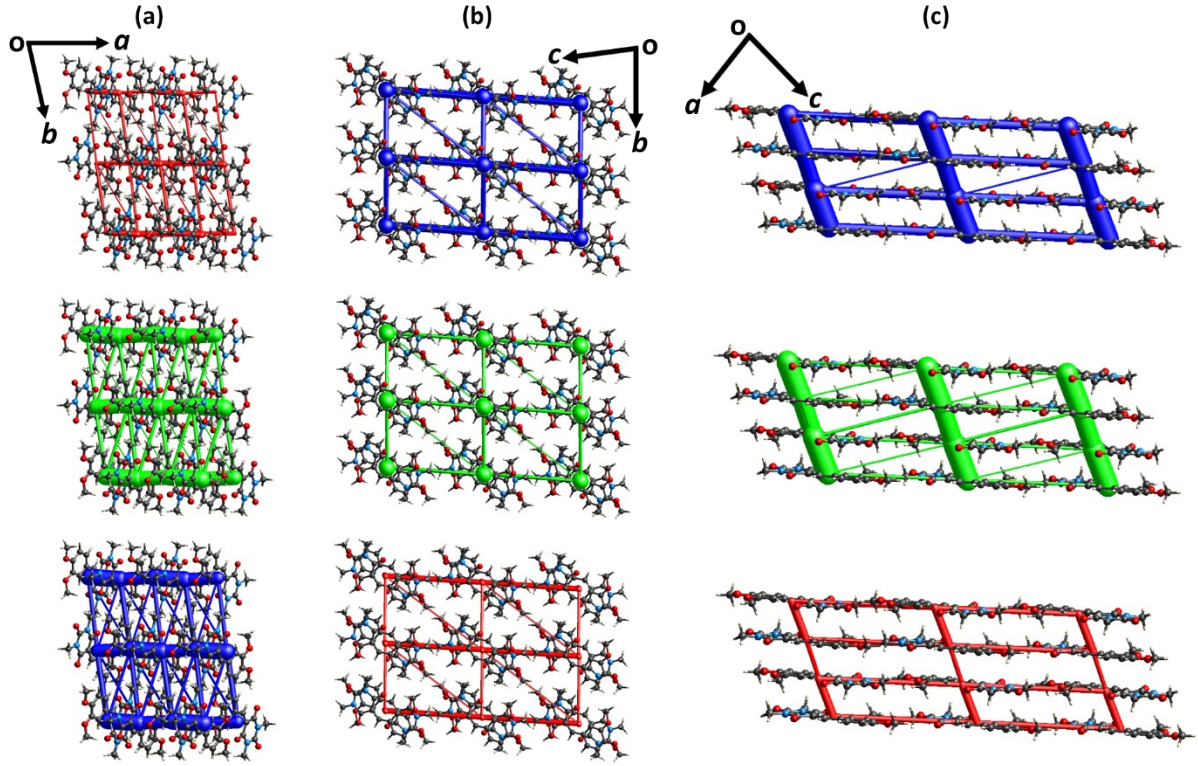

Figure S9. Visualization of energy frameworks showing total interaction energy (top, blue), dispersion (middle, green) and electrostatic (below, red) components crystal **2**, in the **(a)** (001), **(b)** (100) and **(c)** (010) faces, respectively. The energy threshold is 5 kJ.mol^{-1}.

Table S4: (a) Molecular structure pairs and **(b)** the interaction energies (in kJ.mol^{-1}) obtained from energy frameworks calculation for crystal **2**. Scale factors are in the lower table.

(a)

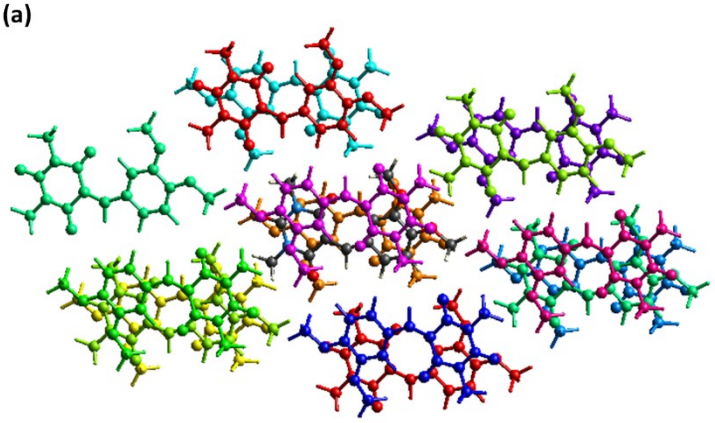

(b) Interaction Energies (kJ/mol)
R is the distance between molecular centroids (mean atomic position) in Å.

Total energies, only reported for two benchmarked energy models, are the sum of the four energy components, scaled appropriately (see the scale factor table below)

N	Symop	R	Electron Density	E_ele	E_pol	E_dis	E_rep	E_tot
2	x, y, z	8.48	B3LYP/6-31G(d,p)	-1.8	-2.5	-18.3	11.3	-12.7
1	-x, -y, -z	3.56	B3LYP/6-31G(d,p)	-32.3	-4.7	-112.5	68.2	-93.4
1	-x, -y, -z	13.89	B3LYP/6-31G(d,p)	-0.4	-0.0	-3.0	0.0	-3.0
2	x, y, z	12.46	B3LYP/6-31G(d,p)	-21.4	-3.1	-16.3	0.0	-39.1
1	-x, -y, -z	11.23	B3LYP/6-31G(d,p)	2.9	-0.2	-15.1	4.3	-7.7
2	x, y, z	14.65	B3LYP/6-31G(d,p)	-5.0	-1.8	-5.8	0.0	-11.7
1	-x, -y, -z	8.19	B3LYP/6-31G(d,p)	-10.2	-2.4	-22.6	13.7	-23.7
1	-x, -y, -z	14.83	B3LYP/6-31G(d,p)	1.1	-0.4	-2.2	0.0	-1.1
1	-x, -y, -z	8.03	B3LYP/6-31G(d,p)	-15.8	-3.8	-22.5	15.2	-29.7
1	-x, -y, -z	11.97	B3LYP/6-31G(d,p)	3.1	-0.4	-8.1	1.7	-3.0
1	-x, -y, -z	3.93	B3LYP/6-31G(d,p)	-17.1	-2.9	-96.6	49.8	-73.6
1	-x, -y, -z	15.87	B3LYP/6-31G(d,p)	-0.7	-0.5	-3.8	0.0	-4.5

Scale factors for benchmarked energy models
See Mackenzie et al. IUCrJ (2017)

Energy Model	k_ele	k_pol	k_disp	k_rep
CE-HF ... HF/3-21G electron densities	1.019	0.651	0.901	0.811
CE-B3LYP ... B3LYP/6-31G(d,p) electron densities	1.057	0.740	0.871	0.618

Molecular Structure and Different Photosalient Behaviour of Compounds 1-4.

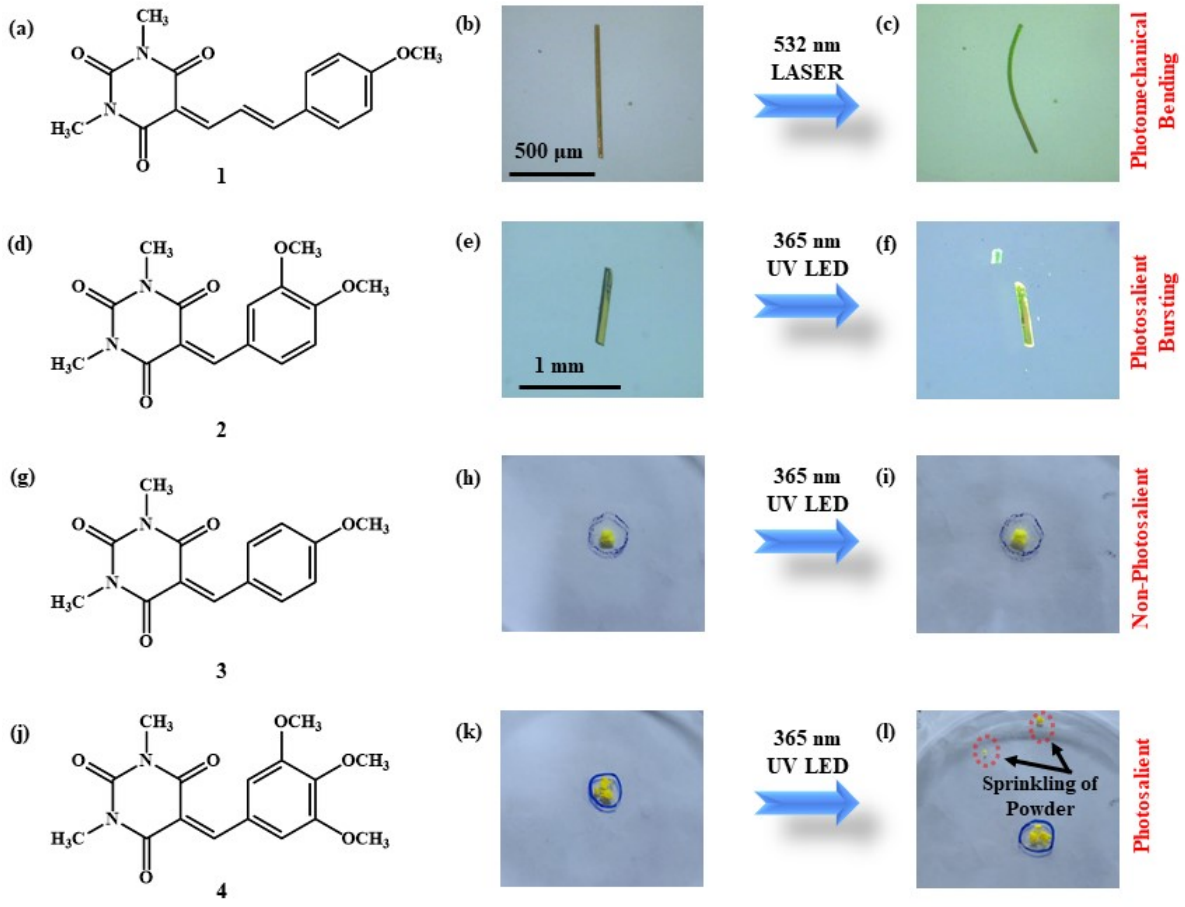

Figure. S10. (a, d, g, j) Molecular structure of compounds **1**, **2**, **3** and **4** respectively, **(b-c)** Crystal of **1** before and after LASER irradiation respectively depicting photomechanical bending, **(e-f)** Crystal of **2** before and after UV irradiation depicting photosalient bursting, **(h-i)** Powder of compound **3** before and after UV irradiation respectively depicting photo-inert nature of **3**, **(k-l)** Powder of **4** before and after UV irradiation respectively depicting photosalient nature of **4**. Blue circle was made with a marker for checking the photoresponses of compounds **3** and **4** in powdered form.

Crystallographic Information Table.

Table S5: Crystallographic information table.

Compound	**Crystal 1**	**Crystal 2**
Formula	$C_{16}H_{16}N_2O_4$	$C_{15}H_{16}N_2O_5$
Molecular Weight	300.31	304.30
T/K	300	298
Crystal System	Triclinic	Triclinic
Space Group	$P\bar{1}$	$P\bar{1}$
a/Å	7.0505(6)	7.456(6)
b/Å	8.0193(7)	8.475(8)
c/Å	13.9507(12)	11.895(16)
α/°	81.526(3)	82.16(6)
β/°	88.415(3)	76.38(5)
γ/°	70.313(3)	71.47(4)
Volume/Å^3	734.36(11)	691.1(13)
Z	2	2
ρ, Mg.cm^{-3}	1.358	1.462
μ /mm^{-1}	0.099	0.111
Reflections Collected	27445	30947
Independent Reflections	3033	2380
R_{int}	0.0395	0.0565
GOF	1.098	1.067
Final R[I>2σ]	0.0664	0.0393
R_1	0.2091	0.1071
wR_2	0.2172	0.1113
CCDC Number	2332071	2324031

References

1. M. J. Turner, S. P. Thomas, M. W. Shi, D. Jayatilaka and M. A. Spackman, *Chem. Commun.*, 2015, **51**, 3735–3738.
2. P. R. Spackman, M. J. Turner, J. J. McKinnon, S. K. Wolff, D. J. Grimwood, D. Jayatilaka and M. A. Spackman, *J. Appl. Crystallogr.*, 2021, **54**, 1006–1011.